

# *ap4b1*<sup>-/-</sup> zebrafish demonstrate morphological and motor abnormalities

Helena Rosengarten<sup>1,2,†</sup>, Angelica D'Amore<sup>1,†</sup>, Hyo-Min Kim<sup>1</sup>, Darius Ebrahimi-Fakhari<sup>1,\*</sup>

<sup>1</sup>Movement Disorders Program, Department of Neurology & The F.M. Kirby Neurobiology Center, Boston Children's Hospital, Harvard Medical School, 300 Longwood Avenue, Boston, MA 02115, United States

<sup>2</sup>Department of Pediatric Neurology, Charité–Universitätsmedizin Berlin, Mittelallee 9, 13353 Berlin, Germany

\*Corresponding author. Department of Neurology, Boston Children's Hospital, 3 Blackfan Circle, Boston, MA 02115, United States.

E-mail: [darius.ebrahimi-fakhari@childrens.harvard.edu](mailto:darius.ebrahimi-fakhari@childrens.harvard.edu)

<sup>†</sup>Helena Rosengarten and Angelica D'Amore contributed equally.

## Abstract

**Objective:** Hereditary spastic paraplegia type 47 (SPG47) is caused by biallelic loss-of-function variants in the AP4B1 gene, leading to neurodevelopmental and progressive motor impairment. This study aimed to generate and characterize a zebrafish (*Danio rerio*) model of SPG47 to investigate the role of *ap4b1* in neurodevelopment and motor function. **Methods:** We employed CRISPR/Cas9 gene-editing to generate a stable *ap4b1*<sup>-/-</sup> zebrafish line. Behavioral, morphological, and motor function analyses were performed, including survival under stress conditions, spontaneous locomotor activity, light–dark transition assays, and coiling behavior. Axonal length was assessed via immunofluorescence targeting spinal motor neurons. Seizure susceptibility was evaluated using a PTZ paradigm. **Results:** *ap4b1*<sup>-/-</sup> zebrafish exhibited significantly reduced axonal length of spinal motor neurons, impaired motor function, and developmental malformations, including brachycephaly, reduced body length, bent spines, and craniofacial defects. Increased tail coiling and reduced spontaneous activity were observed in larvae, alongside absent habituation to light–dark stimuli. Under stress conditions, survival rates were significantly lower in the knockout group compared to controls. Despite early hyperexcitability, no significant increase in PTZ-induced seizures was observed. **Interpretation:** This study characterizes an *ap4b1*<sup>-/-</sup> zebrafish model that recapitulates some phenotypes of SPG47, including motor deficits and morphological abnormalities. These findings support the utility of zebrafish for studying AP-4 deficiency and provide a platform for investigating the molecular mechanisms underlying SPG47.

**Keywords:** hereditary spastic paraplegia; adaptor protein complex 4; zebrafish; axon outgrowth

## Introduction

Hereditary spastic paraplegias (HSPs) are a heterogeneous group of over 80 monogenic disorders and represent the most common cause of inherited spasticity and disability [1]. The hallmark clinical feature of HSP is progressive spasticity and weakness, with childhood-onset forms frequently associated with neurodevelopmental features. Biallelic loss-of-function variants in the AP4B1 gene cause hereditary spastic paraplegia type 47 (SPG47), a rare, childhood-onset, complex form of HSP. SPG47 is characterized by progressive spasticity, global developmental delay and later intellectual disability, epilepsy, postnatal microcephaly, developmental brain malformations, foot deformities, and short stature [2–5].

AP4B1 encodes the beta subunit of the adapter protein complex 4 (AP-4), a crucial component in the trafficking of transmembrane proteins [6]. Recent studies have identified the autophagy protein ATG9A and the endocannabinoid-producing enzyme DAGLB as key cargos of AP-4 [7–11]. Despite the growing understanding of the underlying disease mechanisms, no treatments are currently available to halt disease progression in SPG47.

As is the case for many forms of HSP, the discovery of novel therapeutics for SPG47 has been hindered by the slow disease progression in mouse models, their unsuitability for large-scale *in vivo* screens, and their relatively high costs. Zebrafish (*Danio rerio*) offer an alternative, providing key advantages to overcome these limitations. *Ap4b1* in zebrafish shares approximately 70%

homology with human AP4B1 and is ubiquitously expressed, with robust expression in the central nervous system. Building on prior work using acute knockdown of *ap4s1* in zebrafish larvae via anti-sense oligonucleotides [12], we now report the generation of a stable *ap4b1* knockout zebrafish line through CRISPR/Cas9-mediated introduction of early truncating variants (*ap4b1*<sup>-/-</sup>). Systematic characterization of this knockout line revealed reduced survival under stress conditions and a range of morphological anomalies, including brachycephaly, shortened body length in larvae, bent spines, tail fin defects, and craniofacial deformities in both larval and adult stages. Additionally, we observed behavioral abnormalities, such as increased tail coiling and reduced spontaneous locomotor activity. Consistent with prior findings, we identified shortened axonal length in spinal neurons of developing *ap4b1*<sup>-/-</sup> larvae, highlighting early developmental deficits, impaired motor function, and morphological alterations as core phenotypes of AP-4 deficiency in zebrafish.

## Results

### *ap4b1*<sup>-/-</sup> zebrafish exhibit reduced survival under stress conditions and morphological abnormalities

Zebrafish larvae carrying a homozygous frameshift variant in exon 2 of *ap4b1* (Fig. 1A, Supplementary Fig. 1A and B, *ap4b1*<sup>-/-</sup>) were studied under two survival conditions: normal density

(non-stress) and crowded conditions (stress) from days post-fertilization (dpf) 1 to 5. No significant difference in survival was observed between the *ap4b1*<sup>-/-</sup> larvae and wildtype group (*ap4b1*<sup>+/+</sup>) under non-stress conditions (Fig. 1B). However, under stress conditions, a significant reduction in survival was noted in the *ap4b1*<sup>-/-</sup> larvae. At 5 dpf, the mean survival rate was 17.7 ± 5.51% (SD) for *ap4b1*<sup>-/-</sup> larvae, compared to 64.7 ± 7.1% (SD) for *ap4b1*<sup>+/+</sup> (Fig. 1C).

A comprehensive morphological analysis of 6 dpf larvae raised under normal conditions revealed reduced growth in the *ap4b1*<sup>-/-</sup> group, with decreased total length and nose-to-neck length compared to the *ap4b1*<sup>+/+</sup> group (Fig. 1D and E). The brachycephaly index (ratio of nose-to-neck length to head size) was significantly reduced in the *ap4b1*<sup>-/-</sup> group (Fig. 1F). Measurements evaluating microcephaly (ratio of head size to body length) or head size showed no significant differences between the groups (Fig. 1G and H). Likewise, no significant difference was observed in the nose-to-neck length to body length ratio between the two groups (Fig. 1I).

Considering the physical malformations identified during the larval stage, an in-depth morphological assessment of *ap4b1*<sup>-/-</sup> fish raised to adulthood was conducted. The frequency of three phenotypes was evaluated in the *ap4b1*<sup>-/-</sup> group compared to *ap4b1*<sup>+/+</sup> controls: spinal curvature, tail fin defects, and craniofacial defects. Bent spines were observed more frequently in the *ap4b1*<sup>-/-</sup> population across multiple time points and generations compared to *ap4b1*<sup>+/+</sup>. Notably, the number of animals exhibiting the bent spine phenotype increased over time in both the knockout and wildtype populations. However, the increase in the *ap4b1*<sup>+/+</sup> population was more gradual and uniform across all time points. In contrast, the number of *ap4b1*<sup>-/-</sup> animals with bent spines remained relatively stable between the 7- and 10-month time points, with a significant increase observed at 14 months (Fig. 1J). At 7 months, the number of fish with tail fin defects was roughly equal in both groups. However, by 10 months, more *ap4b1*<sup>-/-</sup> fish exhibited the defect compared to the *ap4b1*<sup>+/+</sup> group. The frequency of this phenotype decreased in both groups compared to the 7-month timepoint. At 14 months, the pattern observed at 10 months persisted, with a significantly higher percentage of the population displaying the phenotype (Fig. 1K). Craniofacial defects were observed in less than 5% of *ap4b1*<sup>+/+</sup> fish across all time points. In contrast, *ap4b1*<sup>-/-</sup> fish with craniofacial defects represented 5% of the mutant population at 7 months, with this percentage rising over time, reaching 30% at 14 months (Fig. 1L).

In a quantitative analysis, we observed that *ap4b1*<sup>-/-</sup> fish were smaller in both body length and width compared to *ap4b1*<sup>+/+</sup> controls across all time points and for both sexes (Fig. 1M and N). The nose-to-neck length of *ap4b1*<sup>-/-</sup> fish was shorter at all time points compared to controls (Fig. 1O), suggesting that AP4-deficient zebrafish generally have a reduced head size. Additionally, *ap4b1*<sup>-/-</sup> fish were proportionally thinner across all time points and generations compared to *ap4b1*<sup>+/+</sup>. Interestingly, the width-to-body length ratio decreased over time in the knockout group compared to the wildtype group (Fig. 1P). A similar trend was observed in tail fin length proportions, where *ap4b1*<sup>-/-</sup> fish consistently had shorter tail fins relative to body size compared to *ap4b1*<sup>+/+</sup> at all 7 and 10 months (Fig. 1Q). The ratio of nose-to-neck length to body length showed no significant difference between the 7- and 10-month populations, but a significant reduction was noted at 14 months (Fig. 1R).

## ***ap4b1*<sup>-/-</sup> zebrafish larvae show abnormal motor behavior**

Early developmental characteristics in our model were assessed by examining tail coiling behavior during the larval stage. By 24 h post-fertilization (hpf), larvae exhibit tail coils, which are brief bursts of tail movement lasting approximately 1 second each. We found that the proportion of time spent coiling was significantly higher in the *ap4b1*<sup>-/-</sup> group compared to *ap4b1*<sup>+/+</sup> (Fig. 2A and B), suggesting an early developmental motor abnormality, possibly related to hyperexcitability.

Spontaneous motor activity at 5 dpf was evaluated by measuring the distance moved over 30 minutes, both in the presence and absence of a light stimulus. The *ap4b1*<sup>-/-</sup> group exhibited significantly reduced spontaneous activity compared to the *ap4b1*<sup>+/+</sup> group in both light and dark phases, indicating lower baseline locomotor activity (Fig. 2C). To further assess behavioral and locomotor responses, we introduced light-dark transitions with a shorter duration of the dark phase (10 minutes instead of 30 minutes) and a reduced light stimulus (5 minutes instead of 30 minutes). In the first round of testing, the *ap4b1*<sup>-/-</sup> group exhibited significantly less movement than *ap4b1*<sup>+/+</sup> in both light and dark phases. However, in the second round, reduced activity in the knockout group was only observed in the absence of light stimulus, suggesting a reduced response to light in the mutants (Fig. 2D). To assess habituation to the light-dark stimuli, we conducted repeated rounds of stimulation and measured the distance moved by the larvae. There was no significant difference in the overall response between the *ap4b1*<sup>-/-</sup> and *ap4b1*<sup>+/+</sup> group (Fig. 2E). However, when analyzing each genotype separately, the *ap4b1*<sup>+/+</sup> group showed a progressive reduction in movement from rounds 2 through 4 compared to round 1, consistent with habituation. In contrast, the *ap4b1*<sup>-/-</sup> group did not show this attenuation, suggesting impaired habituation in the mutants (Fig. 2F). Overall, these findings suggest that *ap4b1* deficiency leads abnormal motor development and activity at an early developmental stage.

## ***ap4b1*<sup>-/-</sup> zebrafish larvae do not show spontaneous seizures or a reduced seizure threshold**

To investigate whether the model exhibited a lower threshold for spontaneous or induced seizures, we performed PTZ challenges. At baseline, around 40% of larvae in both genotypes exhibited normal activity (phase zero), while 5% of larvae from each group displayed slight hyperactivity (phase one). No fish from either group exhibited spontaneous seizure behavior (Fig. 2G). Upon exposure to PTZ, *ap4b1*<sup>-/-</sup> larvae showed an increased, though not statistically significant, trend in phases zero to three (Fig. 2H).

## **Length of spinal motor neurons is reduced in *ap4b1*<sup>-/-</sup> zebrafish larvae**

To investigate potential differences in neurodevelopment and axonal maintenance in the *ap4b1* knockout, we performed immunofluorescence staining targeting *znp-1* (anti-syt2), which marks spinal motor neurons. Axon length in the *ap4b1*<sup>-/-</sup> group was significantly shorter compared to the *ap4b1*<sup>+/+</sup> controls (Fig. 3A), indicating reduced axon growth or potentially impaired axonal maintenance. Furthermore, the axonal projections in the *ap4b1*<sup>-/-</sup> group appeared less organized and more fragmented compared to controls, evident in 3D reconstructions (Fig. 3B). These findings support an axon outgrowth deficiency,

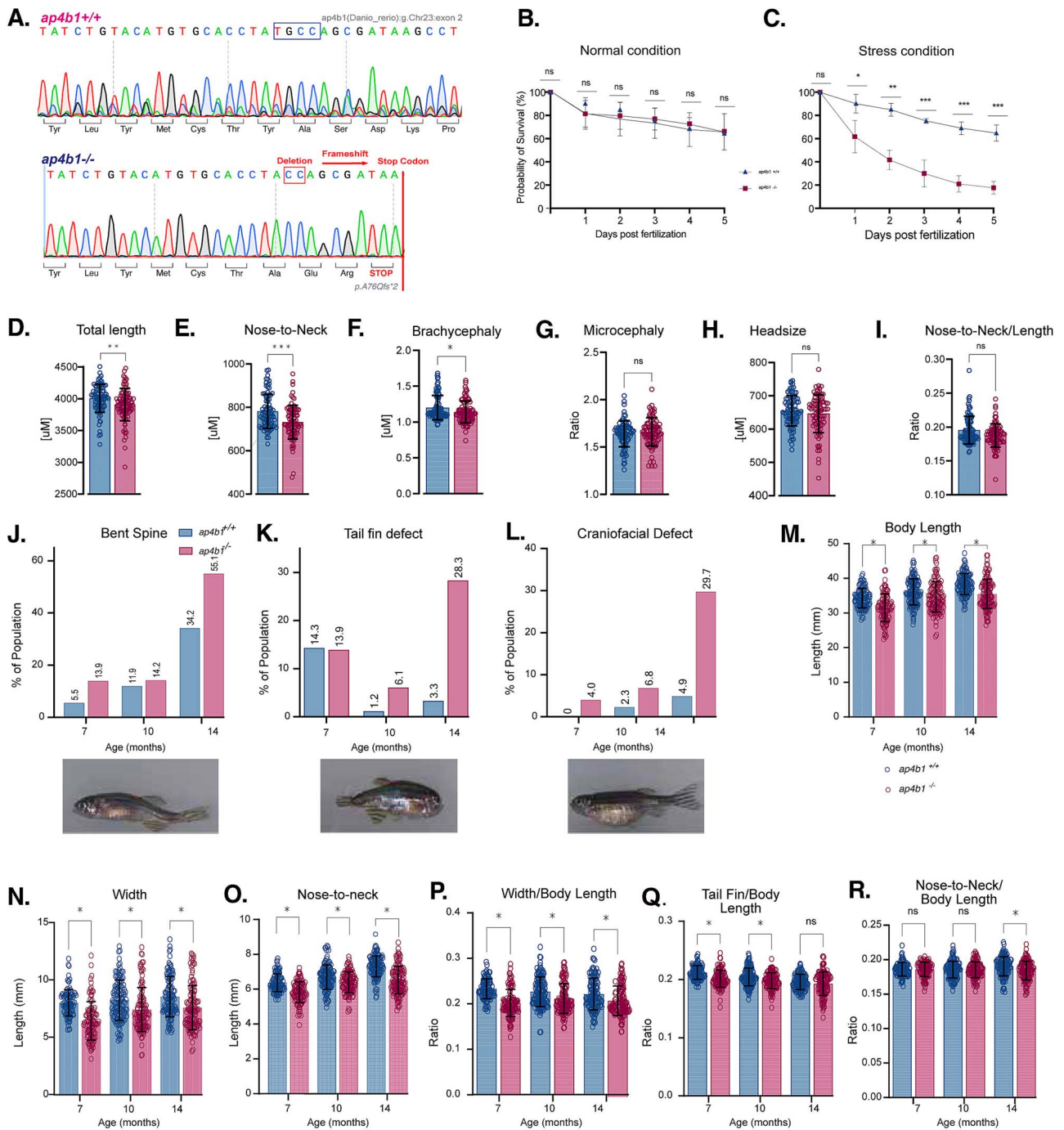


**Figure 1.** Survival and morphology analysis of CRISPR/Cas9-induced *ap4b1* knockout zebrafish. (A) Sanger sequencing confirms an intragenic deletion and subsequent frameshift mutation in the *ap4b1*<sup>-/-</sup> zebrafish line (bottom), compared to *ap4b1*<sup>+/+</sup> (top). The arrow indicates the deletion site. (B and C): Survival analysis was conducted in both mutant and control groups from 1 dpf to 5 dpf under normal housing conditions (left panel), showing no significant reduction in survival in *ap4b1*<sup>-/-</sup> (KO) when compared to *ap4b1*<sup>+/+</sup> (WT). However, when stress housing conditions are applied (>200 eggs per dish; right panel), the probability of survival decreases in *ap4b1*<sup>-/-</sup> when compared to *ap4b1*<sup>+/+</sup>. Each experiment was repeated five times with *n* = 200 eggs per dish under stress conditions and *n* = 80 eggs per dish under normal housing conditions. Data are presented as mean ± standard deviation. Statistical significance between groups at each timepoint was determined using multiple unpaired t-tests with correction for multiple comparisons (ns: *P* > 0.05, \*\*\**P* < 0.001). (D–I) Graphs show the measurements taken to assess morphological anomalies at the larval stage (6 dpf). The data are plotted in the following order: Head size, body length, nose-to-neck length, brachycephaly index, microcephaly, and the ratio between nose-to-neck length and body length. Data are presented as median with error bars indicating the interquartile range, statistical significance between groups was determined using Mann–Whitney test, *n* = 86 WT/KO for body length; *n* = 88 both groups for the other set of measurements, \**P* < 0.05, \*\**P* < 0.01, \*\*\**P* < 0.001]. (J–R) morphological studies were conducted on adult fish from both *ap4b1*<sup>-/-</sup> (KO) and *ap4b1*<sup>+/+</sup> (WT) groups at three different time points (7, 10, and 14 months old), focusing on the following features: Bent spine (Fig. 1J), tail fin defects (Fig. 1K), and craniofacial defects (Fig. 1L). The number of individuals assessed for each time point was as follows: 7 months, *n* = 99 WT, *n* = 100 KO; 10 months, *n* = 126 WT, *n* = 111 KO; 14 months, *n* = 120 WT, *n* = 122 KO. Quantitative measurements taken to assess adult morphology include the following: Body length (Fig. 1M), body width (Fig. 1N), nose-to-neck length (Fig. 1O), width or tail fin divided by body length (Fig. 1P and Q), and nose-to-neck length divided by body length (Fig. 1R). The number of fish assessed for each timepoint was as follows: 7 months, *n* = 99 WT, *n* = 100 KO; 10 months, *n* = 126 WT, *n* = 111 KO; 14 months, *n* = 120 WT, *n* = 122 KO. Data are presented as mean ± standard deviation. Statistical significance between groups was determined using unpaired t-test with \**P* < 0.05. For both qualitative and quantitative analysis, two populations from separate generations were surveyed twice, contributing to both the 10 and 14-month timepoints.

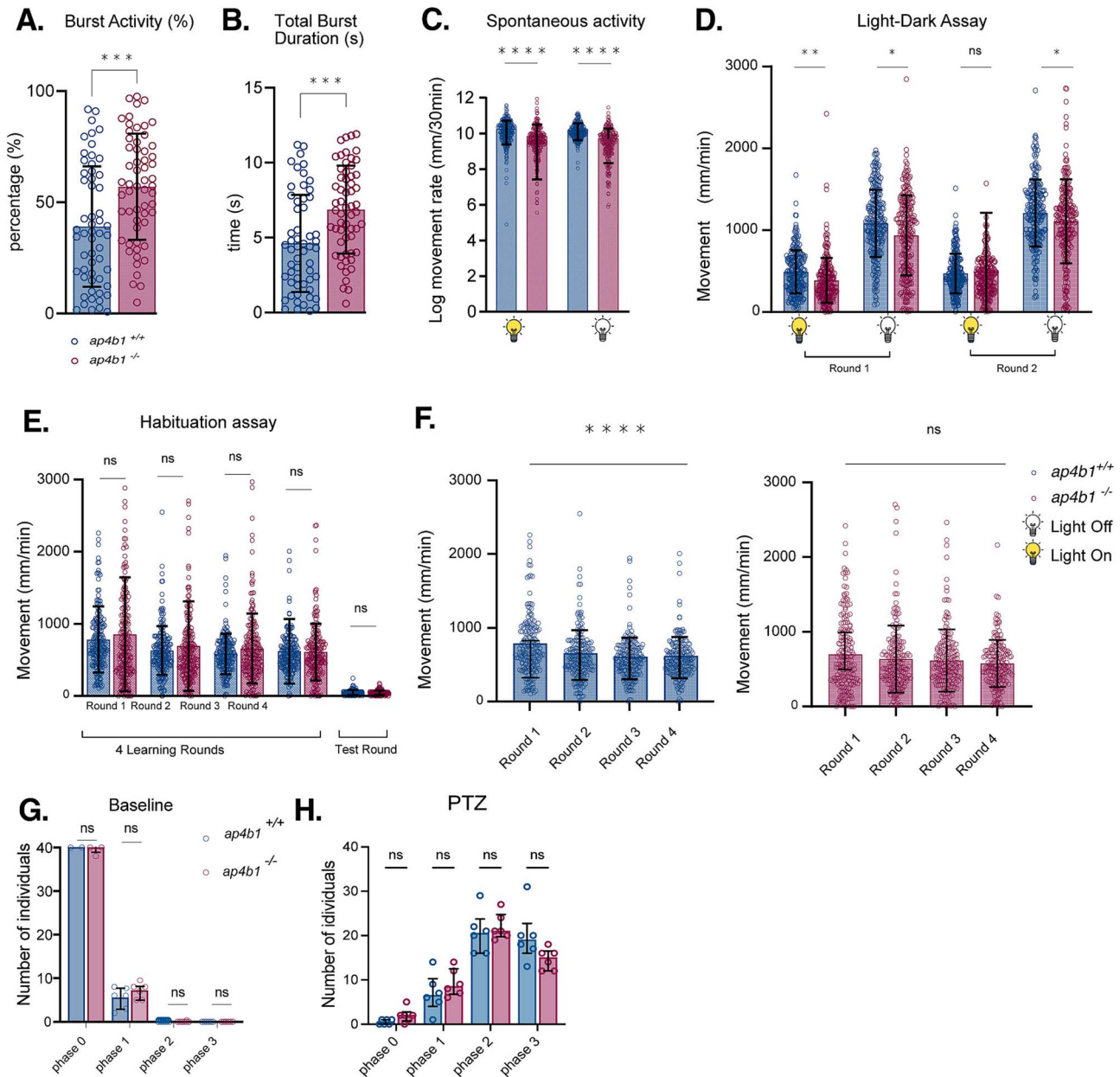


**Figure 2.** Behavioral, motor, and molecular abnormalities in *ap4b1*<sup>-/-</sup> zebrafish. (A and B) to identify potential early developmental abnormalities in the *ap4b1*<sup>-/-</sup> zebrafish, a coiling analysis was performed. Each coiling event or burst was counted, and data were shown as burst activity (percentage of bursts) and total burst duration in seconds. Data are presented as median with error bars indicating the interquartile range; statistical significance between groups was determined using Mann-Whitney test,  $n = 60$  for both groups,  $***P < 0.001$ . (C and D) To test for locomotor impairments, spontaneous activity was observed using the DanioVision system, both in the presence and absence of a light stimulus. Behavioral and locomotor activity of the *ap4b1*<sup>-/-</sup> versus *ap4b1*<sup>+/+</sup> was further tested in a light-dark paradigm with multiple shorter rounds of alternating light-dark stimuli. Data are presented as median with error bars indicating the interquartile range; statistical significance between groups was determined using Mann-Whitney test,  $n = 240$ ,  $*P < 0.05$ ,  $**P < 0.01$ ,  $****P < 0.0001$ . (E and F) To test the learning ability of the *ap4b1*<sup>-/-</sup> zebrafish, a set of experiments was performed to test habituation. Habituation was measured as the distance moved per minute in four learning rounds and one shorter test round, comparing *ap4b1*<sup>+/+</sup> and *ap4b1*<sup>-/-</sup>. There was no significant difference in the overall response between the *ap4b1*<sup>-/-</sup> and *ap4b1*<sup>+/+</sup> groups across all rounds. However, when analyzing each genotype separately, the *ap4b1*<sup>+/+</sup> group showed a progressive reduction in movement from rounds 2 through 4 compared to round 1, consistent with habituation. In contrast, the *ap4b1*<sup>-/-</sup> group did not show this attenuation, suggesting impaired habituation. Data are presented as median with error bars indicating the interquartile range; statistical significance between groups was determined using Kruskal-Wallis one-way analysis of variance,  $n = 192$  for both groups,  $****P < 0.0001$ . (G and H) the frequency and severity of PTZ-induced seizures were scored in 7 dpf larvae. Baseline (G) and post-PTZ administration (H) recordings were taken and subsequently analyzed. Scoring was as follows: Phase 0—no seizure, phase 1—Limited seizure-like behavior, phase 2—Early seizure stage phenotype, phase 3—Severe seizure-like phenotype. Scoring was done by a blinded observer. Six trials were performed on six different clutches, with  $n = 288$  for both knockout and wildtype groups. The number of zebrafish larvae exhibiting a given phase from a single trial is represented as a dot. Data are presented as median with error bars indicating the interquartile range; statistical significance between groups was determined using Mann-Whitney test, ns = not significant.

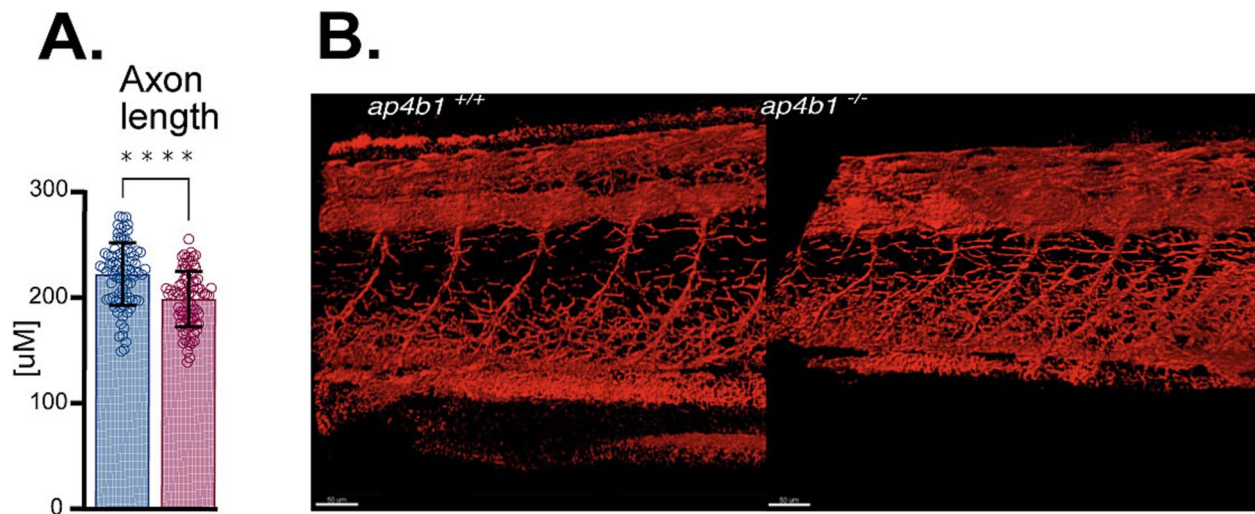


**Figure 3.** Shorter axonal length and disorganized axonal offspring were observed in *ap4b1*<sup>-/-</sup> zebrafish. (A) Znp-1 immunofluorescence staining was performed to investigate morphological changes of spinal motor neurons. Shorter axonal lengths were observed in *ap4b1*<sup>-/-</sup> zebrafish larvae compared to *ap4b1*<sup>+/+</sup> controls (left). Data are presented as mean with error bars indicating the standard deviation,  $n = 87$  axons in the KO group,  $n = 93$  axons in the WT group, unpaired t-test \*\*\*\* $P < 0.0001$ . (B) Representative images show the axonal distribution in *ap4b1*<sup>+/+</sup> versus *ap4b1*<sup>-/-</sup> zebrafish.

consistent with the phenotype observed with a prior antisense oligonucleotide-based acute knockdown [12].

## Discussion

In this study, we generated a stable *ap4b1*<sup>-/-</sup> zebrafish model using CRISPR/Cas9 technology to investigate the underlying mechanisms of SPG47. This model allowed us to explore key phenotypes associated with AP-4 deficiency, including impaired motor function, axonal abnormalities, and developmental malformations. Our findings contribute to the growing understanding of AP-4-related HSPs and underscore the potential utility of zebrafish as a model for studying these disorders.

One of the most significant findings of this study is the reduction in axonal length observed in *ap4b1*<sup>-/-</sup> zebrafish larvae. This phenotype aligns with previous reports of axonal degeneration in other AP-4-related HSP models [7–10, 13] and highlights the critical role of the AP-4 complex in supporting axonal growth and maintenance. The disorganization and fragmentation of axonal projections in *ap4b1*<sup>-/-</sup> larvae further underscore the neurodevelopmental impairments associated with AP-4 deficiency [2, 3, 5]. Along with these morphological changes, our findings also uncovered motor and behavioral abnormalities in the *ap4b1*<sup>-/-</sup> zebrafish. The increased tail coiling observed during early development suggests hyperexcitability in the neuronal network, which may contribute to the motor deficits seen later in life. The reduced spontaneous locomotor activity in both light and dark conditions point to a general decrease in baseline motor function. Interestingly, the lack of habituation to repeated light–dark transitions in the knockout group may suggest an underlying learning or cognitive impairment. Beyond neuronal function, *ap4b1*<sup>-/-</sup> zebrafish also exhibited significant morphological defects, including reduced body length, brachycephaly, craniofacial deformities, and bent spines. These anomalies were present in both larval and adult stages, suggesting that AP-4 deficiency affects multiple stages of development. The increased prevalence of skeletal malformations, including bent spines, in older *ap4b1*<sup>-/-</sup> zebrafish may reflect the progressive nature of SPG47, where motor dysfunction and spasticity worsen over time. Surprisingly, despite the common presence of seizure

in SPG47 patients, the *ap4b1*<sup>-/-</sup> zebrafish did not exhibit a significant increase in seizure susceptibility in the PTZ assay. This discrepancy between the zebrafish model and human epilepsy phenotypes could reflect species-specific differences in seizure susceptibility or neural circuitry. Further investigation, such as adding a thermal stress paradigm or recording local field potentials to assess seizure-like spikes, would provide additional insights into the neurophysiological changes associated with AP-4 deficiency.

Although the *ap4b1*<sup>-/-</sup> zebrafish model does not fully recapitulate all human features of SPG47, it may offer a platform for investigating the molecular underpinnings of these impairments and for testing potential interventions aimed at improving motor function. The ability to generate large numbers of animals per spawn and the rapid life cycle of zebrafish make them particularly well-suited for medium throughput drug screening. While zebrafish provide several advantages as a model system, including their optical transparency, high fecundity, and rapid development, there are also important limitations to consider. To minimize off-target effects, we selected sgRNAs with the lowest predicted off-target binding and designed three sgRNAs in the initial round. However, we cannot fully exclude the possibility of off-target effects contributing to the observed phenotype. A related limitation is that genetic compensation and/or altered RNA processing around the indel site—previously reported in CRISPR/Cas9-generated indel mutants [14]—could result in incomplete gene knockout and an attenuated phenotype. This may explain differences compared to the *ap4s1* knockdown line generated using morpholino technology [12].

The lack of specific antibodies for zebrafish proteins, such as AP-4 subunits and cargo such as ATG9A, limits the tools available for probing AP-4 related protein trafficking. This hinders the depth of mechanistic studies, particularly when investigating complex downstream pathways like autophagy. Future studies may overcome this challenge by utilizing transgenic reporter lines or developing novel antibodies. Prior work in AP-4-deficient cells [7] and *Ap4b1* knockout mice [15, 16] suggests that effects of AP-4 deficiency on autophagic flux are subtle and may be tissue-specific. Consequently, detecting these changes in larval zebrafish tissue—considering developmental context and limited

tissue availability—may be particularly challenging. Beyond biochemical phenotypes, the high degree of variability in behavioral and developmental phenotypes among zebrafish populations can make it difficult to detect subtle differences between mutant and wildtype groups, particularly when considering the quality metrics needed for high-throughput screens. While the zebrafish model is valuable for studying early neurodevelopmental disorders, the absence of cortical structures in zebrafish limits their utility for modeling higher-order cognitive functions and epilepsy. As such, findings from zebrafish models may serve as a first screen that allows more targeted testing in mammalian systems.

In summary, our stable *ap4b1*<sup>-/-</sup> zebrafish line recapitulates some of the features of SPG47, including motor deficits, axonal shortening, and structural abnormalities. This model provides a platform for studying the underlying mechanisms of AP-4 deficiency and for testing potential therapeutic interventions. The insights gained from this study highlight the critical role of AP-4 in neurodevelopment and motor function and set the stage for future mechanistic investigations.

## Materials and methods

All zebrafish experiments described here were approved by the Institutional Animal Care and Use Committee (IACUC) at Boston Children's Hospital (IACUC #00001775). Detailed methods are provided in [Supplementary File 1](#) and additional data is included in [Supplementary Fig. 1](#).

## Acknowledgements

The authors thank Dr Barbara Robens (Poduri Lab) and the staff at the Aquatic Resources Program at Boston Children's Hospital for help in setting up the *ap4b1*<sup>-/-</sup> zebrafish line. The authors thank Annapurna Poduri, M.D., MPH (Boston Children's Hospital) and Angela Kaindl, MD (Charité—Universitätsmedizin Berlin) for guidance and support. This work was funded by the Cure AP-4 Foundation.

## Supplementary data

[Supplementary data](#) is available at *HMG Journal* online.

**Conflict of interest statement:** The authors report no relevant conflicts of interest.

## Funding

This work as supported by research grants from the NIH/NINDS (K08NS123552-01) and the CureAP4 Foundation (both to D.E.F.).

## References

- Shribman S, Reid E, Crosby AH. et al. Hereditary spastic paraplegia: from diagnosis to emerging therapeutic approaches. *Lancet Neurol* 2019;**18**:1136–1146.
- Ebrahimi-Fakhari D, Alecu JE, Ziegler M. et al. Systematic analysis of brain MRI findings in adaptor protein complex 4-associated hereditary spastic paraplegia. *Neurology* 2021;**97**:e1942–e1954.
- Alecu J, Schierbaum L, Ebrahimi-Fakhari D. AP-4-Associated Hereditary Spastic Paraplegia. 2018 Dec 13 [updated 2025 Feb 6]. In: Adam MP, Feldman J, Mirzaa GM, Pagon RA, Wallace SE, Amemiya A, (eds). *GeneReviews*<sup>®</sup> [Internet]. Seattle (WA): University of Washington, Seattle; 1993–2025.
- Ebrahimi-Fakhari D, Cheng C, Dies K. et al. Clinical and genetic characterization of AP4B1-associated SPG47. *Am J Med Genet A* 2018;**176**:311–318.
- Ebrahimi-Fakhari D, Teinert J, Behne R. et al. Defining the clinical, molecular and imaging spectrum of adaptor protein complex 4-associated hereditary spastic paraplegia. *Brain* 2020;**143**:2929–2944.
- Mattera R, De Pace R, Bonifacino JS. The role of AP-4 in cargo export from the trans-Golgi network and hereditary spastic paraplegia. *Biochem Soc Trans* 2020;**48**:1877–1888.
- Behne R, Teinert J, Wimmer M. et al. Adaptor protein complex 4 deficiency: a paradigm of childhood-onset hereditary spastic paraplegia caused by defective protein trafficking. *Hum Mol Genet* 2020;**29**:320–334.
- Davies AK, Alecu JE, Ziegler M. et al. AP-4-mediated axonal transport controls endocannabinoid production in neurons. *Nat Commun* 2022;**13**:1058.
- Mattera R, Park SY, De Pace R. et al. AP-4 mediates export of ATG9A from the trans-Golgi network to promote autophagosome formation. *Proc Natl Acad Sci USA* 2017;**114**:E10697–E10706.
- Ivankovic D, Drew J, Lesept F. et al. Axonal autophagosome maturation defect through failure of ATG9A sorting underpins pathology in AP-4 deficiency syndrome. *Autophagy* 2020;**16**:391–407.
- Davies AK, Itzhak DN, Edgar JR. et al. AP-4 vesicles contribute to spatial control of autophagy via RUSC-dependent peripheral delivery of ATG9A. *Nat Commun* 2018;**9**:3958.
- D'Amore A, Tessa A, Naef V. et al. Loss of ap4s1 in zebrafish leads to neurodevelopmental defects resembling spastic paraplegia 52. *Ann Clin Transl Neurol* 2020;**7**:584–589.
- Saffari A, Brechmann B, Boger C. et al. High-content screening identifies a small molecule that restores AP-4-dependent protein trafficking in neuronal models of AP-4-associated hereditary spastic paraplegia. *Nat Commun* 2024;**15**:584.
- Salanga CM, Salanga MC. Genotype to phenotype: CRISPR gene editing reveals genetic compensation as a mechanism for phenotypic disjunction of Morphants and mutants. *Int J Mol Sci* 2021;**22**:3472.
- Scarrott JM, Alves-Cruzeiro J, Marchi PM. et al. Ap4b1-knockout mouse model of hereditary spastic paraplegia type 47 displays motor dysfunction, aberrant brain morphology and ATG9A mislocalization. *Brain Commun* 2023;**5**:fcac335.
- Wiseman JP, Scarrott JM, Alves-Cruzeiro J. et al. Pre-clinical development of AP4B1 gene replacement therapy for hereditary spastic paraplegia type 47. *EMBO Mol Med* 2024;**16**:2882–2917.